EFDA–JET–CP(09)05/010

M. Vrancken, E. Lerche, T. Blackman, P. Dumortier, F. Durodié, M. Evrard, R.H. Goulding, M. Graham, S. Huygen, P. Jacquet, A. Kaye, M.-L. Mayoral, M.P.S. Nightingale, J. Ongena, D. Van Eester, M. Van Schoor, M. Vervier, R. Weynants and JET EFDA contributors

Operational Experience with the Scattering Matrix Arc Detection System on the JET ITER-Like Antenna

Operational Experience with the Scattering Matrix Arc Detection System on the JET ITER-Like Antenna

M. Vrancken[1], E. Lerche[1], T. Blackman[2], P. Dumortier[1], F. Durodié[1], M. Evrard[1], R.H. Goulding[3], M. Graham[2], S. Huygen[1], P. Jacquet[2], A. Kaye[2], M.-L. Mayoral[2], M.P.S. Nightingale[2,b] J. Ongena[1], D. Van Eester[1], M. Van Schoor[1], M. Vervier[1], R. Weynants[1] and JET EFDA contributors*

JET-EFDA, Culham Science Centre, OX14 3DB, Abingdon, UK

[1]*LPP/ERM-KMS, Association EURATOM-Belgian State, Brussels, Belgium*
[2]*EURATOM-UKAEA Fusion Association, Culham Science Centre, OX14 3DB, Abingdon, OXON, UK*
[3]*Oak Ridge National Laboratory, Oak Ridge, United States*
** See annex of F. Romanelli et al, "Overview of JET Results",*
(Proc. 22[nd] IAEA Fusion Energy Conference, Geneva, Switzerland (2008)).

Preprint of Paper to be submitted for publication in Proceedings of the
18th Topical Conference on Radio Frequency Power in Plasmas, Gent, Belgium.
(22nd June 2009 - 24th June 2009)

ABSTRACT.

The Scattering Matrix Arc Detection System (SMAD) has been fully deployed on all 4 sets of Resonant Double Loop (RDL), Vacuum Transmission Line (VTL) and Antenna Pressurised Transmission Lines (APTL) of the JET ICRF ITER-Like Antenna (ILA) and this has been indispensable for operating at low (real) T-point impedance values to investigate ELM tolerance. This paper describes the necessity of the SMAD vs VSWR (Voltage Standing Wave Ratio) protection system, SMAD commissioning, problems and a number of typical events detected by the SMAD system during operation on plasma.

1. INTRODUCTION

Figure 1 shows the position of the measurement points of the 4 independent SMAD [1] arc detection systems on the left half of the ILA [2] denoted as E12,E34 (symmetrical right half E56,E78 not shown). Each $SMAD_{kl}$ system (kl) = (12), (34), (56), (78) the directional coupler forward and reflected voltages V^+_{kl}, V^-_{kl} at the APTL (Antenna Pressurised Transmission Line) and the RF pickup probe total voltages V_k, V_l at the fixed capacitor flange (start of strap feeder) and produces an error signal [1]

$$SMAD_{kl} = \frac{K_{1kl}.V_k + K_{2kl}.V_l}{V_{kl}^- - K_{3kl}.V_{kl}^+} \tag{1}$$

with error coefficients $K_{ikl}(S_{3x3}(f),C_k,C_l,f)$ (i=1,2,3) determined from the RF model [1] $S_{3x3}(f)$ matrix, measured capacitor values C_k,C_l and operating frequency f. The standard VSWR protection system relies on the MTL (Main Transmission Line)

$VSWR_{kl}$ at the generator side (see Fig.1). The SMAD system complements the VSWR protection to detect arcs in the low impedance T-point region [2], [3] where the sensitivity of the VSWR system decreases. Fig. 2 shows an RF circuit simulation with a "representative" plasma load matrix (from TOPICA simulation [4]) that illustrates this point. In a fully matched ($Re(Z_{Tkl}) = 3\Omega$) and fully balanced array (equal capacitor voltage amplitudes $|V_k/V_l| = 1$, and $|V_2/V_3| = |V_2/V_6| = 1$) ($Im(Z_{Tkl})$ then follows from the plasma load and imposed generator phasing), the position of all matching elements are frozen and a parallel arc $L_p = 20nH$ (between central and outer conductor RF ground) is inserted and moved along the length of the VTL of E12 as shown in Fig.1. This mimics the situation where an arc suddenly occurs at that position and modifies the voltages and currents over the entire system while the matching system has had no time to adjust itself. Figure 2 shows that the $SMAD_{12}$ error signal detects the presence of the arc around the T-point (fraction ~0), while the $VSWR_{12}$ signal is high for arcs occurring at the back of the VTL (fraction ~1) where the impedance is high, but becomes insensitive around the T-point region where the impedance decreases to 3Ω. The simulation also shows that this particular equation for the $SMAD_{kl}$ error signal has an insensitive zone in the middle of the VTL (fraction 0.20-0.65 for this threshold 0.35), but that his area is protected by the VSWR system. Also note that the arc on E12 alters the voltage/ current distribution over the entire system due to mutual coupling over the front strap array, and this causes the $VSWR_{34}$ to rise while all other $SMAD_{kl}$ (kl) = (34), (56), (78) error signals remain 0. This simulation thus also illustrates the difficulty of interpreting real trip events because in reality the hardware is wired such that any single $VSWR_{kl}$ or $SMAD_{kl}$ event trips all generators at the same time.

2. SMAD COMMISSIONING ISSUES

It is important to mention some difficulties encountered in commissioning the SMAD hardware. Initial operation on plasma with $Re(Z_T = 6\Omega)$ revealed that the signals in the SMAD PC [1] had to be re-identified and re-arranged for correct error calculation. Subsequently, threshold levels for the individual signals V_k, V_l, V^+_{kl}, V^-_{kl} (around ~10kV) and the net forward power (~20kW) at which a "healthy" SMAD error signal is calculated were determined experimentally to allow recovery after a trip. Loss of the internal potentiometer of capacitor C_2 was a problem for $SMAD_{12}$ but the weak dependence of the coefficients on capacitor values allowed to copy the readback of the toroidal neighbour capacitor C_6, leaving the SMAD for E12 more sensitive nevertheless. First operation on H-mode showed tripping on all ELMs but this was quickly traced to different bandwidths among electronics processing the RF signals before entering the SMAD PC [1].

3. SMAD EVENTS AND ARC DETECTION

Figure 3(a) shows relevant signals and thresholds for JET Pulse No. 75946 with the lower half ILA at 42MHz increasing power from 1.0MW to 2.0MW during L-mode and reducing back to 1.0MW during the remaining ELMy H-mode. In the RF pulse with $Re(Z_{Tkl}) = 6\Omega$ and capacitor voltages not fully balanced [5], the $SMAD_{34}$ and SHAD (SubHarmonic Arc Detection [6]) error and logical trip signals are produced but not yet connected to the generator trip system. The $SMAD_{34}$ error signal is depicted with the original coefficients used on this pulse (COEF1) and with coefficients (COEF2) optimized over a range of operating conditions (L-, H-mode and ELMs). Fig.3(b) shows a time zoom (13.6-13.67s), where an asymmetric change of the capacitor voltages (13.62s) accompagnies a VSWR trip. Since the event is not detected by the SMAD, this is most likely an arc on the strap connected to capacitor C_3. On reapplication of the power (13.64s) the SMAD error signal with original coefficients (COEF1) does not decrease fast enough and would have tripped the system, while the optimized set of coefficients (COEF 2) would not have. Again at full power, a clear arc detected by the SMAD (13.65s) initiates an oscillation that dies out and is suspected to be related to the inner strap phase control feedback system [5]. Fig. 3(c) shows the timezoom 16.62-16.72s. At the first ELM (16.63s), the VSWR does not reach the trip limit thanks to the ELM resilience and the second stage "offset" match [5], but the SMAD error signal clearly detects an arc. At 16.665s, VSWR and SHAD [6] system confirm an arc, but the SMAD error remains low indicating an arc outside the SMAD monitored region. The SMAD shows the same problem on power reapplication at 16.67s as in Figure 3(b). Finally, all arc detection systems are well behaved during the second ELM (16.72s) as is the case with the majority of ELMs over the entire pulse.

CONCLUSIONS

This paper has described first results of the 4 SMAD arc detection systems on the JET-ILA and its interaction with the existing VSWR trip system. Some problems encountered during commissioning were described and experimental VSWR, SMAD and SHAD events described. The system has protected the ILA during $Re(Z_T) = 3\Omega$ operation although a full evaluation of its performance relative to the other systems would require a more detailed and overall statistical analysis over all shots which is still outstanding.

ACKNOWLEDGMENTS

This work, supported by the European Communities under the contract of Association between EURATOM and Belgian state and between EURATOM and UKAEA, was carried out within the framework of the European Fusion Development Agreement. The views and opinions expressed herein do not necessarily reflect those of the European Commission. The work carried out by UKAEA personnel was also funded by the United Kingdom Engineering and Physical Sciences Research Council.

REFERENCES

[1]. M. Vrancken et al., Fusion Engineering Design **84**, 1953-1960 (2009).
[2]. F. Durodié et al., Fusion Engineering Design **74**, 223-228 (2005).
[3]. F. Durodié et al., These Proceedings.
[4]. V. Lancellotti et al., Nuclear Fusion **46**, S476-S400 (2006).
[5]. M. Vrancken et al., These Proceedings.
[6]. P. Jacquet et al., These Proceedings.

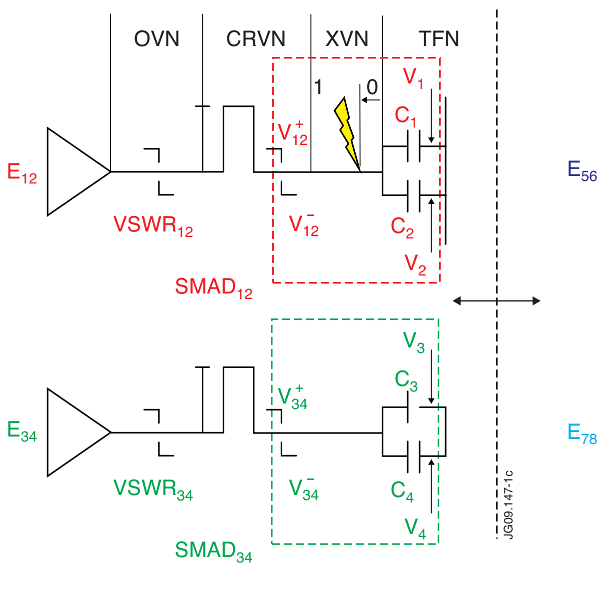

Figure 1: Left half ILA system E12, E34 with measurement positions for $SMAD_{kl}$ (V^+_{kl}, V^-_{kl}, V_k, V_l) and $VSWR_{kl}$ (at generator side) protection systems. Right half E56, E78 is toroidally symmetrical.

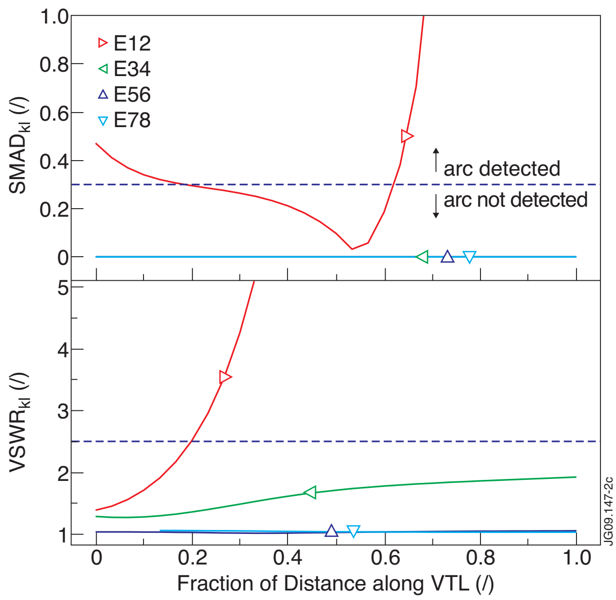

Figure 2: $SMAD_{kl}$ and $VSWR_{kl}$ signals as function of position of L_p=20nH arc along E12 VTL for a fully matched array with $Re(Z_T)$=3Ω and equal amplitude capacitor voltages. Arcs with L_p<20nH would decrease the extent of the unprotected zones.

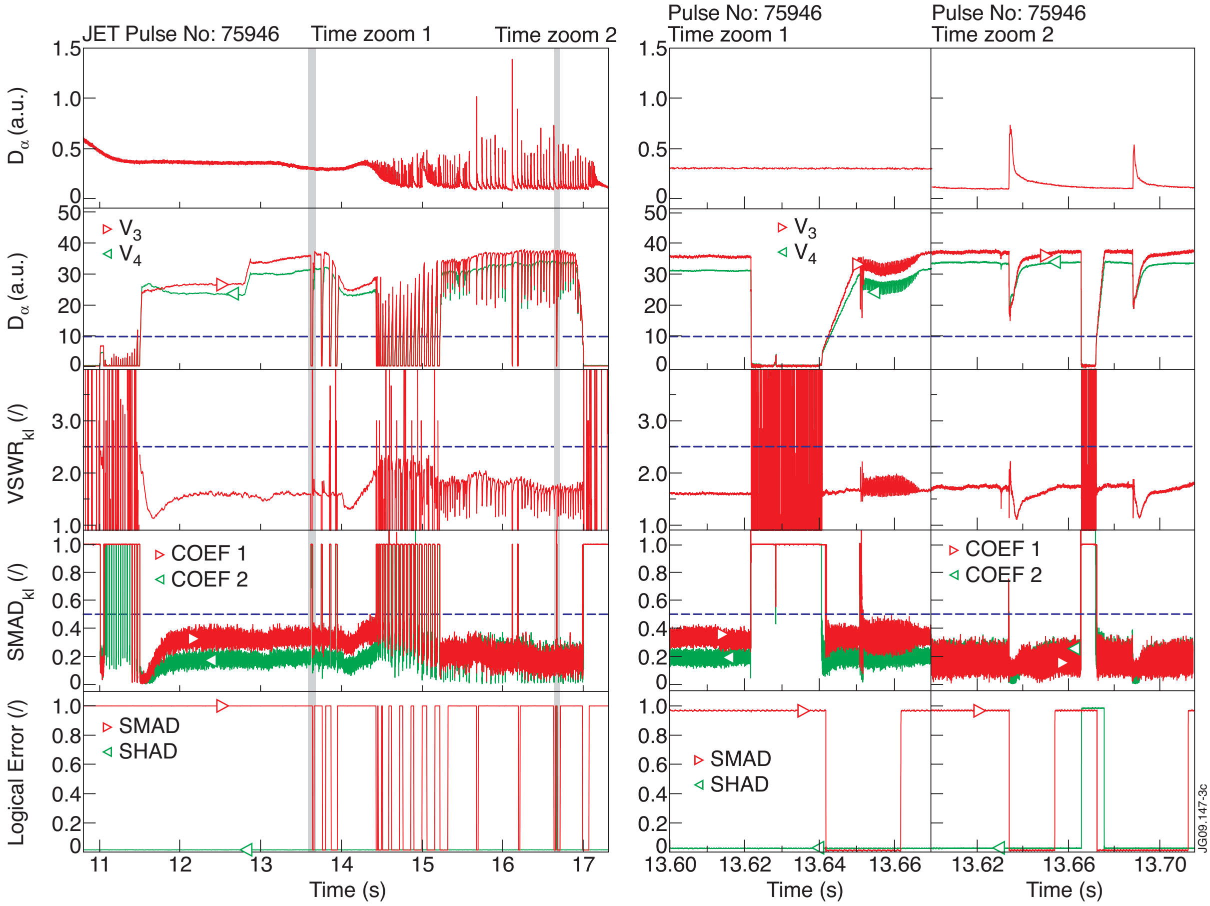

*Figure 3: (a) ILA lower half RF pulse at 42*MHz *from 11-17*s *during JET Pulse No. 75946, with $D_\pm$ ELM signal, capacitor voltages V_3,V_4, $VSWR_{34}$ (threshold 2.5), $SMAD_{34}$ error signal from original coefficients (COEF1, threshold 0.5) and optimized coefficients (COEF2, threshold could be lowered to ~0.35) and SMAD (failsafe arc=0) and SHAD (arc=1) logical trip signals. (b) Time zoom 13.6-13.67*s. *(c) Time zoom 16.62-16.72*s.